NASA TN D-123

TECHNICAL NOTE
D-123

INVESTIGATION OF THE EFFECT OF A GUIDE-VANE—ROTOR COMBINATION ON INLET TOTAL-PRESSURE DISTORTIONS IN A COMPRESSIBLE FLUID

By George C. Ashby, Jr.

Langley Research Center
Langley Field, Va.

NATIONAL AERONAUTICS AND SPACE ADMINISTRATION
WASHINGTON
December 1959

NATIONAL AERONAUTICS AND SPACE ADMINISTRATION

TECHNICAL NOTE D-123

INVESTIGATION OF THE EFFECT OF A GUIDE-VANE—ROTOR COMBINATION ON INLET TOTAL-PRESSURE DISTORTIONS IN A COMPRESSIBLE FLUID

By George C. Ashby, Jr.

SUMMARY

An experimental investigation has been conducted in a compressible fluid to determine the effectiveness of having a 90° included angle between the absolute- and relative-flow directions at the inlet of a compressor in reducing an inlet total-pressure distortion. The total-pressure distortion produced by a 31-percent open plate was measured upstream and downstream of the rotor of a guide-vane—rotor combination which was designed to have a 90° included angle at all radial stations. For these tests the average relative Mach number was 0.65 and the average density ratio across the rotor was approximately 1.12.

The distortion was greatly reduced across the rotor. Comparison of the downstream measured distortion with that estimated by using the recovery ratio equations of Smith (Transactions American Society of Mechanical Engineers, April 1958) shows that the magnitude of the distortion behind the rotor was estimated with reasonable accuracy by the equation for an incompressible fluid.

INTRODUCTION

High-speed turbojet aircraft are confronted with operating problems resulting from nonuniform distributions of total pressure and velocity at the entrance to the compressor. The causes, the effects, and the means of reducing the flow distortions are discussed in reference 1.

Reference 1 points out that the various means of reducing the distortion before it reaches the compressor result in weight, volume, and/or pressure recovery penalties. In addition, the compressor has to operate in some distortion, since it is not completely eliminated by these methods. Reference 1 also indicates that, for an incompressible fluid, velocity diagrams having an included angle of 90° between the relative- and absolute-flow directions at either the inlet or exit of the rotor are

optimum for eliminating inlet total-pressure distortions within the first stage of the compressor.

The purpose of the present investigation was to check the effectiveness of a 90° included angle in attenuating a distortion in a compressible fluid. A distortion plate extending over 1/6 (60°) of the circumference of the annulus was inserted upstream of the guide vane and measurements of the flow were made upstream and downstream of a rotor in a guide-vane—rotor combination having an included angle of approximately 90° at all radial stations. The measured results were compared with values calculated by using the equations given in reference 2.

SYMBOLS

a	velocity of sound, ft/sec
h	static enthalpy, ft^2/sec^2
H	total enthalpy, ft^2/sec^2
M	Mach number
P	total pressure, lb/sq ft
dP	total-pressure difference between undistorted flow and point in distorted flow, lb/sq ft
r	radius measured from axis of compressor, ft
U	blade speed, ft/sec
V	velocity, ft/sec
φ	flow coefficient, V_a/U
α	angle of attack relative to blade chord $\beta_{1R} - \xi$, deg
β	flow angle measured from axis of rotation, deg
ξ	blade setting angle (angle between chord and axis of rotation), deg
η	polytropic efficiency
σ	solidity, blade chord divided by blade gap

Subscripts:

i	upstream of guide vane
1	upstream of rotor
2	downstream of rotor
a	axial direction
d	design conditions
R	relative coordinates
r	root
t	tip

ANALYSIS FOR AN INCOMPRESSIBLE FLUID

The significance of having a 90° included angle between the relative- and absolute-flow directions at either the inlet or exit of a rotor is explained in detail in reference 1. However, for the benefit of the reader a brief explanation is given here.

The following sketch shows the circumferential velocity profile of a flow with a distortion entering a compressor rotor blade row.

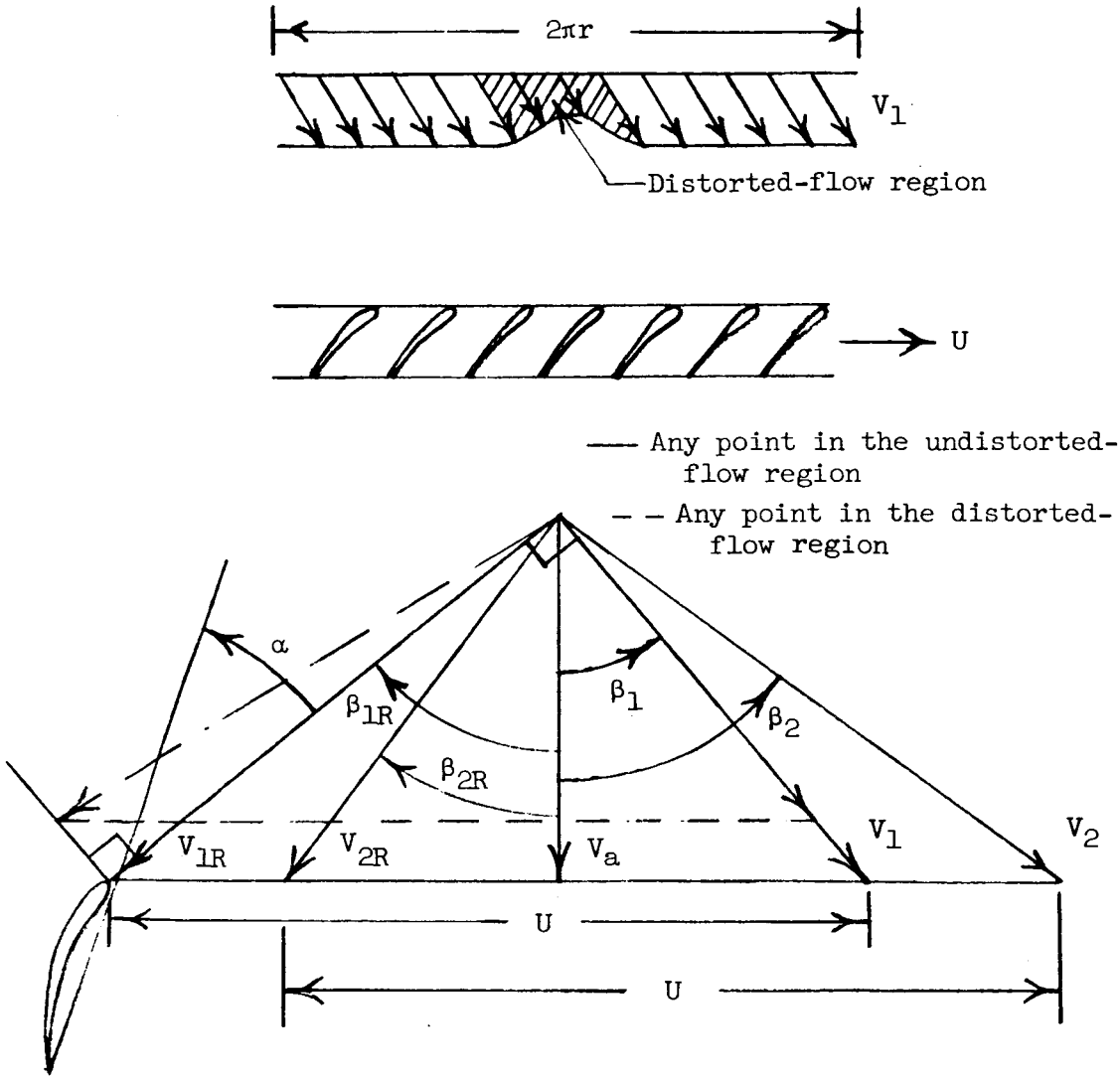

The velocity diagram of the blade in the distorted-flow region is superimposed on the velocity diagram of the blade in the undistorted-flow region. With the included angle $\beta_{1R} + \beta_1$ equal to 90° the inlet relative-velocity vector V_{1R} of the undistorted flow is perpendicular to the line along which lies the extremities of the inlet relative-flow vector V_{1R} of both flows. Therefore, the inlet relative-flow vectors of both flows are approximately the same length. Assuming an incompressible fluid and the static pressure of the two regions to be equal at the inlet of the rotor makes the total pressure relative to the rotor equal for the two flows. If the losses in the blade passage and the exit directions are assumed to be the same for both flows, it is found that the

relative velocity vectors exiting the rotor V_{2R} are coincident. The rotational velocity U is the same for both flows; therefore, the velocity vectors are also coincident in the absolute frame of reference and the exit total pressures are the same for the two flows. With these assumptions a 90° included angle between the relative- and absolute-flow direction at the inlet of a compressor rotor is the optimum for eliminating inlet total-pressure distortions across the first stage of a compressor. A similar analysis shows the same result for a 90° included angle at the exit of the rotor.

The downstream total-pressure deficit in terms of the upstream deficit and the flow angles is expressed in reference 1 for an incompressible fluid as

$$dP_2 = dP_1\left[\cos(\beta_1 + \beta_{1R})\cos(\beta_2 + \beta_{2R})\frac{\cos\beta_1}{\cos\beta_{1R}}\frac{\cos\beta_{2R}}{\cos\beta_2}\right] \qquad (1)$$

An independent analytical analysis based on slightly different assumptions was conducted in reference 2 for a compressible as well as an incompressible fluid. In the analysis it was assumed that the exit flow direction relative to the rotor β_{2R} is a function of the relative inlet angle β_{1R}, and the efficiency in the rotor was assumed to be the same for both the undistorted and distorted flows; whereas, in reference 1 the exit angle β_{2R} and the loss in the rotor were assumed to be the same for both flows. The other assumptions are the same for both analyses. The equation for the downstream deficit derived in reference 2 is

for a compressible fluid:

$$dP_2 = dP_1\frac{P_2}{P_1}\left(1 - \frac{\eta}{\varphi_2}\frac{h_1}{H_2}\left\{\frac{h_2}{h_1}\sin\beta_{2R}\cos\beta_{2R} + \frac{\varphi_2}{\varphi_1}\sin\beta_1\cos\beta_1 - \frac{\sin\beta_{2R}\cos\beta_{2R}\sin\beta_1\cos\beta_1}{\varphi_1} - \frac{\cos^2\beta_{2R}\cos^2\beta_1}{\varphi_1}\exp\left[-\pi\sigma\left(\cos\beta_{2R} + \frac{1-\cos\beta_{2R}}{1.28}\sigma^{\sec\beta_{2R}}\right)\right]\right\}\right) \qquad (2)$$

and for an incompressible fluid:

$$dP_2 = dP_1\left(1 - \frac{\eta}{\varphi_2}\left\{\sin \beta_{2R} \cos \beta_{2R} + \frac{\varphi_2}{\varphi_1} \sin \beta_1 \cos \beta_1 - \frac{\sin \beta_{2R} \cos \beta_{2R} \sin \beta_1 \cos \beta_1}{\varphi_1} - \frac{\cos^2 \beta_{2R} \cos^2 \beta_1}{\varphi_1} \exp\left[-\pi\sigma\left(\cos \beta_{2R} + \frac{1 - \cos \beta_{2R}}{1.28} \sigma^{\sec \beta_{2R}}\right)\right]\right\}\right) \quad (3)$$

When equation (1) is applied to the present investigation, a zero downstream distortion is predicted because the upstream included angles are approximately 90°. For this reason equations (2) and (3) are used to estimate the downstream distortion.

APPARATUS AND PROCEDURE

Test Apparatus

A schematic drawing of the compressor test stand is presented in figure 1. With the exception of the distortion plate and the rotatable casing, the test facility is the same as that described in reference 3. The 1/8-inch distortion plate had 5/32-inch holes uniformly distributed and, as a result, the plate was 31 percent open. The plate extended 60° circumferentially and was mounted at the top of the annulus 4 inches ahead of the guide vane. (See fig. 2.) In order to facilitate probe measurement over the complete circumferential extent of the distortion, the guide vane was attached to the inner casing, and the outer casing in the region of the compressor stage was free to rotate 360°. The rotatable casing was supported at each end by a shoulder on the adjacent casing. Rotation was accomplished by gearing the casing to an electric motor. Sealing was effected at the fore-and-aft junctions of the casing by means of a circular rubber gasket.

The design details of the rotor are given in reference 4. The rotor blades had NACA A_2I_{8b} mean lines and 65-series thickness distributions. (See ref. 5.) The maximum thickness varied from 8 percent at the tip to 10 percent at the root. The tip diameter was 16 inches and the hub-tip radius ratio was 0.75. The blade chord at the mean radius was 2.199 inches and the solidity was 1.0 from hub to tip.

The guide vane was designed to produce a 90° included angle between the absolute- and relative-flow directions entering the rotor at all radial stations. It was composed of 24 blades having NACA 63-$(c_{l_o} A_4 K_6)$06

airfoil sections (ref. 6). (The part of the designation of these sections within parentheses follows a system used explicitly for compressor and turbine profiles. In this system the number within parentheses represents the design lift coefficient c_{l_o} in tenths. The letters A to K are identified with the mean lines a = 1.0 to a = 0 for each increment of 0.1, and the subscripts indicate the fraction (in tenths) of the lift coefficient associated with the particular mean line.) The following table presents the design details:

Station	r/r_t	Section	α_d, deg	$\beta_{1,d}$, deg	Chord, in.	σ_d
Tip	1.0	$63\text{-}(1.42A_4K_6)06$	16.8	25.8	2.094	1.0
Outboard	.9375	$63\text{-}(1.61A_4K_6)06$	18.8	29.8	2.094	1.067
Mean	.870	$63\text{-}(1.80A_4K_6)06$	21.5	33.4	2.094	1.143
Inboard	.8125	$63\text{-}(2.00A_4K_6)06$	24.4	37.9	2.094	1.231
Hub	.75	$63\text{-}(2.20A_4K_6)06$	27.4	42.9	2.094	1.333

It should be pointed out that the 90° restriction theoretically produces an angle of attack at the rotor tip 2° above design and at the rotor hub 5° below design. However, reference 7 shows that a guide vane having a decreasing circulation from hub to tip, as has the subject guide vane, will have an overturning at the tip and an underturning at the hub due to secondary-flow effects; therefore, the variation from design α at the rotor hub and tip will be somewhat less than indicated. The station 1 design velocity diagrams at the tip, mean, and hub are presented in figure 3. Note that the design included angles $\beta_1 + \beta_{1R}$ are 87.8°, 90°, and 90.4° at the tip, mean, and hub, respectively; however, as stated above, the secondary-flow effects tend to increase the value at the tip and decrease the value at the hub.

Instrumentation

Four iron-constantan thermocouples mounted in the settling chamber were used to determine the inlet stagnation temperature. The inlet total pressure was obtained from an L-shaped total-pressure tube in the settling chamber. The measuring stations are shown in figure 1. Figure 2 shows the instrumentation at each station. Previous experience has shown that the static pressure is uniform at station 1; therefore, wall taps on the inner casing only were used to measure static pressure at that station. A short prism-type probe, described in reference 8, and wall taps were used to measure the static pressure at both stations 1 and 2.

The prism probe, a 5-tube shielded total-pressure rake and a 4-tube double-shielded iron-constantan thermocouple were used to measure flow direction, total pressure, and total temperature, respectively, at stations 1 and 2.

Rotor speed was determined by means of a commercial stroboscopic tuning-fork-controlled instrument. The proportion of gas constituents and the physical characteristics of the Freon-12—air mixture were determined from measurement of the velocity of sound in the mixture. This measurement was made with an instrument similar to that described in reference 9.

All pressures were measured by multiple-tube mercury manometer boards and all temperatures were indicated on a commercial-type self-balancing potentiometer. Constant values of settling-chamber pressure were maintained by an automatic control valve.

Test and Procedure

In actual practice distortions are found to be as high as 20 percent. However, since the present series of tests were designed to determine whether a 90° included angle $\beta_1 + \beta_{1R}$ would be effective in reducing a total-pressure distortion in a compressible fluid, the distortion level was selected so that the angle of attack to the rotor in the distortion region would not be large enough to stall the rotor. The distortion level was determined to be 5 percent.

All tests were made in Freon-12 gas at an equivalent rotor speed of 6,300 revolutions per minute. The relative Mach number M_{1R} varied from 0.5 at the root to 0.8 at the tip. The average density ratio across the rotor was 1.12. The settling-chamber pressure was maintained at approximately 20 inches of mercury absolute. Inlet stagnation temperature varied from 81.5° F to 85° F. The Freon-12 purity by volume was 95.5 percent.

Total-pressure measurements were made at intervals $1/2^\circ$ to 1° apart over a 120° circumferential region. Total temperature, static pressure, and flow direction were measured in positions free of guide-vane wakes. Starting with the survey probe in a given position, the static pressure and flow direction were measured at five radial stations, corresponding to the radial stations of the shielded total-pressure rakes. The outer casing was rotated until the next measuring position for one of the three instruments was reached and that particular measurement was made. This procedure was repeated until the desired values had been measured for the 120° region.

RESULTS AND DISCUSSION

The circumferential total-pressure distributions are plotted as the ratio of the difference between the total pressure of the undistorted flow and a point in the distorted flow to the settling-chamber pressure as a function of circumferential distance measured from the center of the upstream distortion region. Figure 4 presents the circumferential total-pressure distributions measured upstream and downstream of the rotor, together with the downstream distribution estimated by using equations (2) and (3) of reference 2, at five radial positions located at 12.5 percent, 31.25 percent, 50 percent, 68.75 percent, and 87.50 percent of the annulus height. At all radii the upstream included angle $\beta_1 + \beta_{1R}$ is between 91° and 92° while the downstream included angle $\beta_2 + \beta_{2R}$ varies from 86° at the inboard section to 102° at the outboard section. The estimated downstream curves have been shifted to account for the circumferential movement of the flow through the rotor. The flows move approximately 25° clockwise (in a positive direction in fig. 4); therefore, as an examination of the extremities of the downstream estimated distortion will reveal, the distorted-flow region exits the rotor blade in the circumferential regions extending approximately from -11.0° to 57.0°, depending on the radius. It can be seen in figure 4 that at all radii the distortion is greatly reduced and the amount of reduction at each radius is approximately the same.

With the initial point of the downstream distortion 25° clockwise of the initial point upstream, it is observed that some distortion was measured counterclockwise of the downstream initial point. This distortion may be a result of flow deflection due to the presence of the distortion plate which increases the angle of attack of the guide vane and reduces the guide-vane turning. This, in turn, could produce a greater than stall angle of attack to the rotor and therefore less power input in this region of the flow. The loss in power input may be explained as follows: At the initial point of the upstream distortion the flow field in the rotor blade passage is dictated by the flow counterclockwise of this point. If the blade is stalled in this region, the relative velocity will probably be less than that of the distortion region. In order to be in equilibrium with the surrounding pressure field, the flow of the distorted region will have a larger radius of curvature in the blade passage, and therefore the flow will be underturned. This condition would result in a lower power input to the distorted flow than would be obtained when the flow field has been established to conform to the flow conditions in the distorted region.

It is also observed that the downstream distortion decreases in the clockwise direction. This result is possibly due to the time delay in establishing an effective angle of attack equal to the value required by the distorted flow.

In actual practice where the distortion would emanate from the inlet and no distortion plate would be present to deflect the flow, it is believed that the downstream distortion would not occur counterclockwise of the initial point and the magnitude of the downstream distortion would be somewhat lower.

The downstream distortion estimated by using the equation for an incompressible fluid from reference 2 agrees with the measured curve more closely than the distortion estimated by using the equation for a compressible fluid from reference 2. Since in actual practice the flow deflection and the resulting distortion caused by the presence of the distortion plate would not exist, it is seen that the measured distortion level would be reasonably well estimated by the equation for an incompressible fluid of reference 2.

CONCLUSIONS

An experimental investigation has been conducted in a compressible fluid to determine the effectiveness of having a 90° included angle between the absolute- and relative-flow directions at the inlet of a compressor in reducing an inlet total-pressure distortion. As a result of this investigation the following conclusions are made:

1. The guide-vane—rotor combination with inlet included angles of approximately 90° at all radial stations was very effective in reducing the total-pressure distortion.

2. The equation for an incompressible fluid derived by Smith (Transactions American Society Mechanical Engineers, April 1958) estimated the downstream distortion level to a reasonable degree.

Langley Research Center,
National Aeronautics and Space Administration,
Langley Field, Va., July 30, 1959.

REFERENCES

1. Ashby, George C., Jr.: Investigation of the Effect of Velocity Diagram on Inlet Total-Pressure Distortions Through Single-Stage Subsonic Axial-Flow Compressors. NACA RM L57A03, 1957.

2. Smith, Leroy H., Jr.: Recovery Ratio - A Measure of the Loss Recovery Potential of Compressor Stages. Trans. ASME, vol. 80, no. 3, Apr. 1958, pp. 517-524.

3. Bernot, Peter T., and Savage, Melvyn: Transonic Investigation of an Axial-Flow Compressor Rotor With a Hub-Tip Ratio of 0.75 and Blades Having NACA A_2I_{8b} Mean Lines. NACA RM L57H08, 1957.

4. Savage, Melvyn, Erwin, John R., and Whitley, Robert P.: Investigation of an Axial-Flow Compressor Rotor Having NACA High-Speed Blade Sections (A_2I_{8b} Series) at Mean Radius Relative Inlet Mach Numbers up to 1.13. NACA RM L53G02, 1953.

5. Erwin, John R., Savage, Melvyn, and Emery, James C.: Two-Dimensional Low-Speed Cascade Investigation of NACA Compressor Blade Sections Having a Systematic Variation in Mean-Line Loading. NACA TN 3817, 1956. (Supersedes NACA RM L53I30b.)

6. Dunavant, James C.: Cascade Investigation of a Related Series of 6-Percent-Thick Guide-Vane Profiles and Design Charts. NACA TN 3959, 1957. (Supersedes NACA RM L54I02.)

7. Lieblein, Seymour, and Ackley, Richard H.: Secondary Flows in Annular Cascades and Effects on Flow in Inlet Guide Vanes. NACA RM E51G27, 1951.

8. Schulze, Wallace M., Ashby, George C., Jr., and Erwin, John R.: Several Combination Probes for Surveying Static and Total Pressure and Flow Direction. NACA TN 2830, 1952.

9. Huber, Paul W., and Kantrowitz, Arthur: A Device for Measuring Sonic Velocity and Compressor Mach Number. NACA TN 1664, 1948.

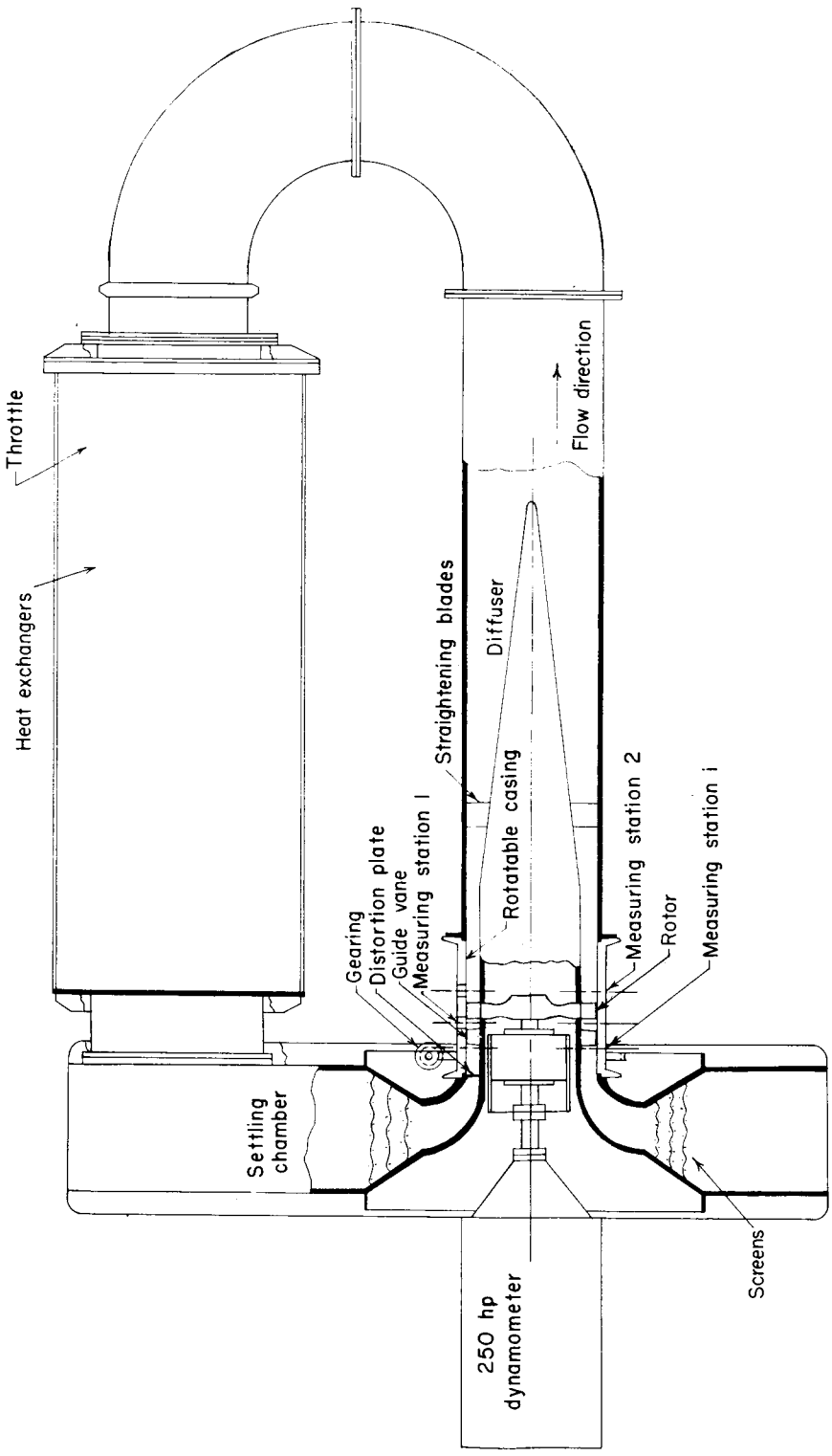

Figure 1.- Schematic drawing of compressor test stand.

L-251

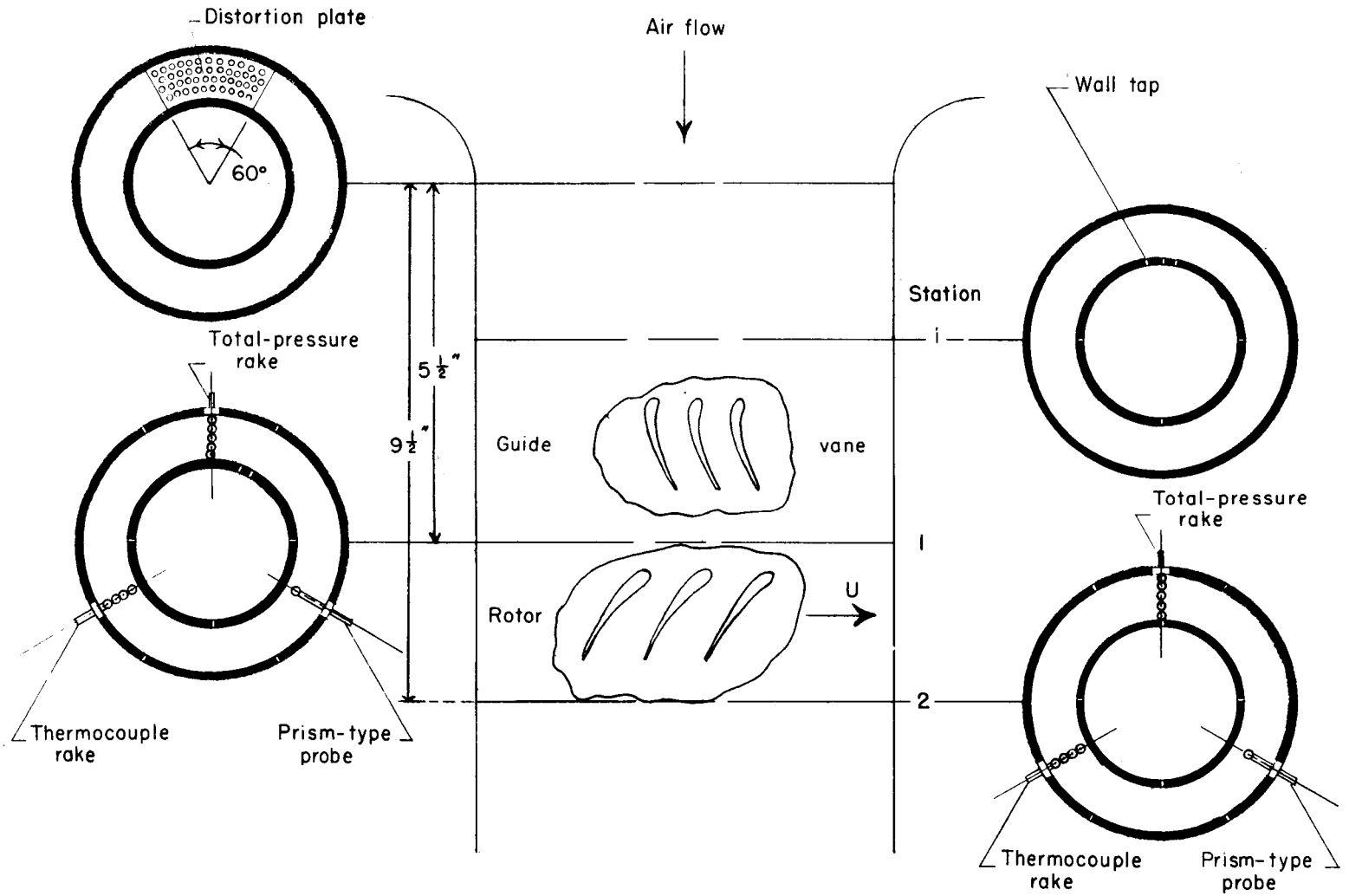

Figure 2.- Location of instrumentation.

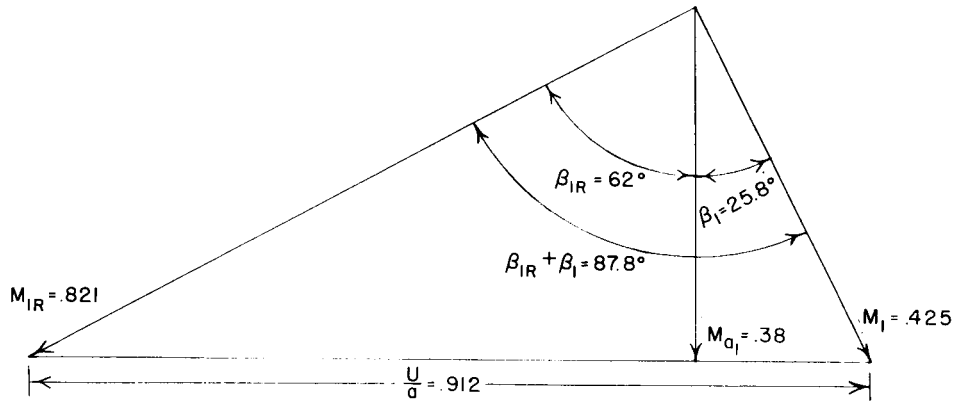

(a) Tip section.

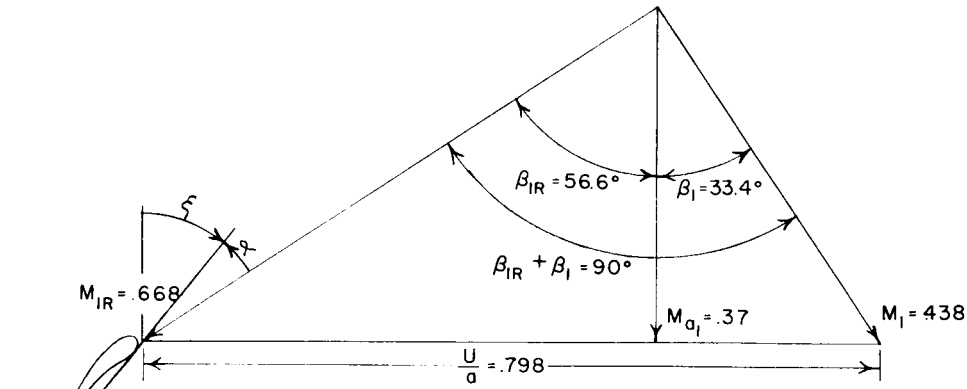

(b) Mean radius section.

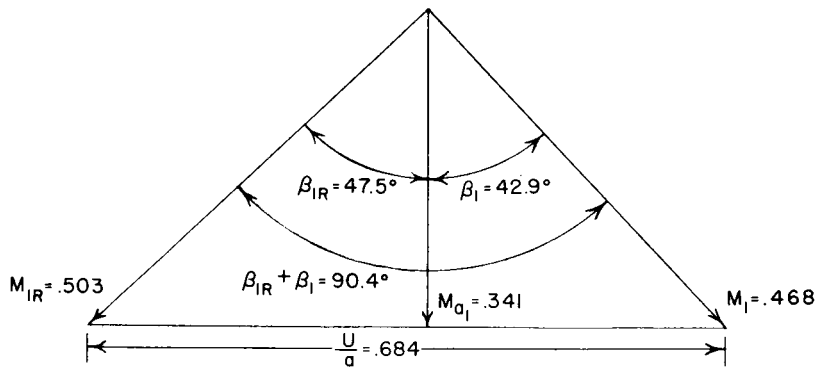

(c) Root section.

Figure 3.- Design velocity diagram at station 1.

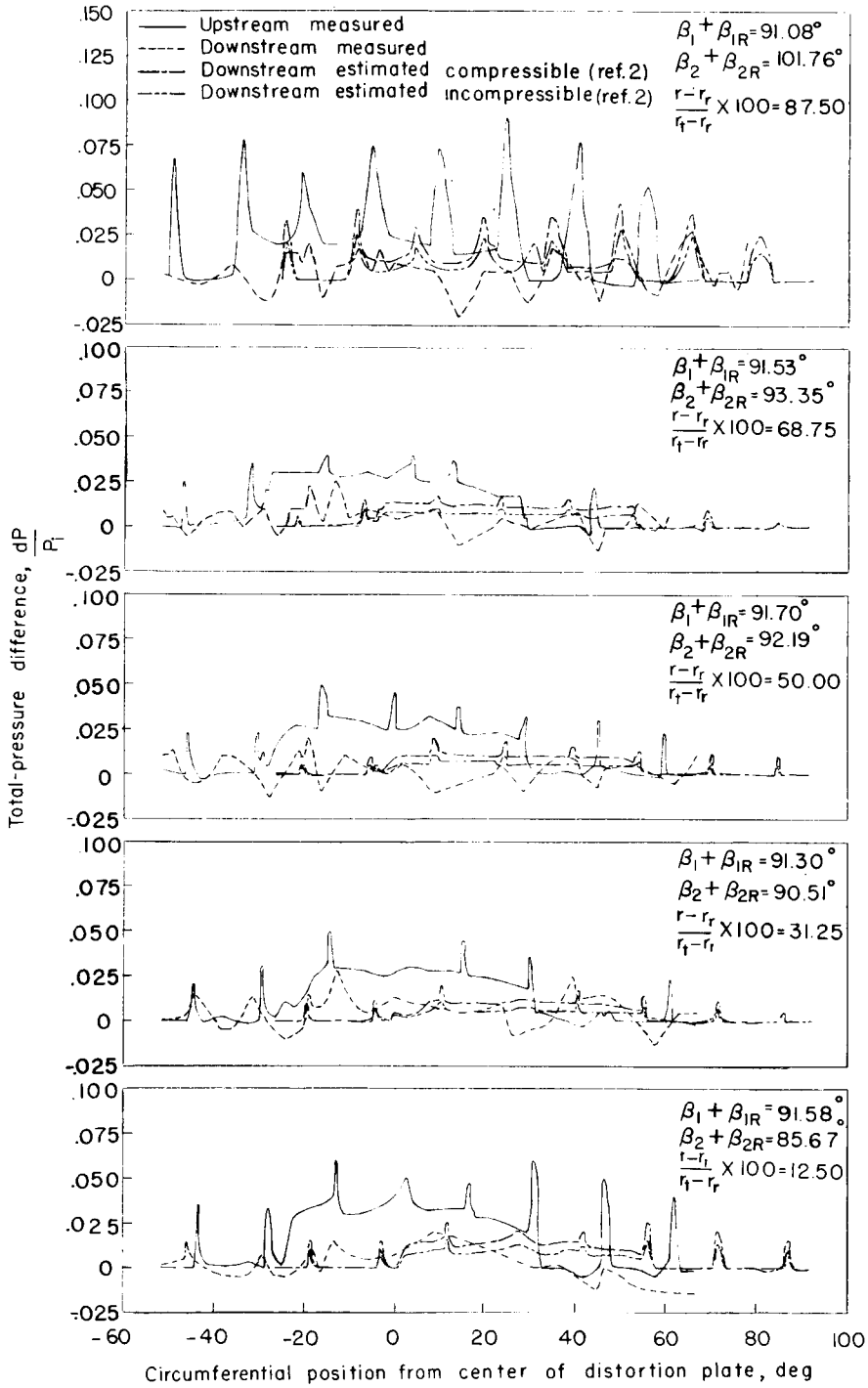

Figure 4.- Comparison of the measured and estimated downstream distortion with the measured upstream distortion at five radial stations.